

Probing the Spatial-temporal Properties of the Nuclear Pore Complex

Affiliation: Division of Natural System, School of Natural Science and Technology, Kanazawa University, Kakuma-machi, Kanazawa 920-1192, Japan.

Author: MAHMOUD SHAABAN MOHAMED ABDELRASOUL

Chief advisor: Prof. Richard Wong

Abstract

Nuclear pore complexes (NPCs) are large protein complexes that span the nuclear envelope. NPCs are the sole gates implanted in the nuclear envelope (NE), acting as a central nano-machine that can regulate the transport between the cytosol and the nucleus. NPCs consist of ~30 proteins, termed nucleoporins. About 30 % of nucleoporins harbor natively unstructured, intrinsically disordered phenylalanine-glycine repeats (FG-Nups), which engage in transport selectivity. NPC structure is well studied by many visualization methods. However, all of these methods were giving static snapshots of NPC to reveal the structure. In this study, I show that high-speed atomic force microscopy (HS-AFM) can be used to directly visualize nanotopographical changes of the nuclear pore central channel in colorectal cancer (CRC) cells. Furthermore, I precisely proposed a tentative biophysical model for the single FG filament bending and extension in healthy and cancer based on my HS-AFM nano-observations and calculations. Therefore, these data revealed new patterns of those intrinsically disordered FG Nups in their native environment. The current HS-AFM observations of native FG Nups provide a tentative explanation of the biophysical motion model of FG Nups inside the central channel. The current data explain how single FG filaments form the central selective network. Furthermore, this model explains how the IDP-FG Nups turnover from one state to another on in the native NPCs. Also, this model revealed that IDP-FG filaments under certain conditions, twist over each other to form a thick aggregates which gradually may form a central granule. Taken together, these results unveiled different nano characteristics of FG Nups in different mammalian cells.

Introduction

The NPC is one of the largest protein complexes in the cell and easily recognizable using electron microscopy (EM). Early EM studies revealed eightfold rotational ring symmetry for the entire structure. In addition, the main NPC structure contains rings that are situated on its cytoplasmic and nucleoplasmic sides, giving the NPC an apparent twofold symmetry through the nuclear envelope. One issue that is agreed upon is that the regulation of the NPC is achieved by specific group of Nups, collectively known as FG-Nups. FG-Nups contain a structured domain that serves as an NPC anchor point, from which an unstructured, filamentous prolongation emanates, which containing many hydrophobic phenylalanine–glycine (FG)-repeats. To be precise, nucleocytoplasmic transport in vivo proceeds through NPCs in a scale of milliseconds. Therefore, it is the dynamic spatiotemporal behaviour of the FG Nups rather than their static time-independent properties that regulate the NPC selective barrier. Yet very little is understood about FG Nup dynamics - in time and space terms- given the lack of techniques that can visualize and probe their time-dependent behaviour inside the native NPCs.

Several key advantages make high-speed AFM (HS-AFM) beneficial for observing NPCs in action. First, stable tapping-mode imaging can be aqueous solutions at low piconewton forces using small cantilevers and nonlinear feedback. Second, the tapping force is applied in microsecond pulses, which minimizes disturbances to the FG Nups as the transfer impulse is very small. Third, at the most rapid scanning speeds, HS-AFM movies are able to capture dynamic nanoscale movements at ~ 100 ms frames per second.

Hypothesis

The spatiotemporal dynamics of mammalian NPCs are not accessible within the previous studies due to technical limits; in the current study I used the HS-AFM to visualize the nanotopomorphological conformations of native NPCs. Because, HS-AFM can record the individual protein complex dynamics on the nanoscale. Recent study used HS-AFM to visualize the nano-dynamics of NPCs in *Xenopus* eggs. However, NPC dynamics in mammalian and/or cancer cells yet to be revealed. Typically, all of the signaling pathways which promote cancer metastasis and progression enter the nucleus through the NPC. Therefore, in the current study, I focused to use human cancer cells as a model to study the native dynamics of NPC. In addition, previous studies has not reveal the structural dynamic differences between normal and cancer cells on the nano-sclae resolution. So, using the same methodology I compared the main structural differences between normal and cancer colon NPC. This comparison also showed the selective barrier of the pore. Furthermore, I gave deep measurements of the single FG Nup filaments since their motion model still under investigations due to technical limits.

Key Results

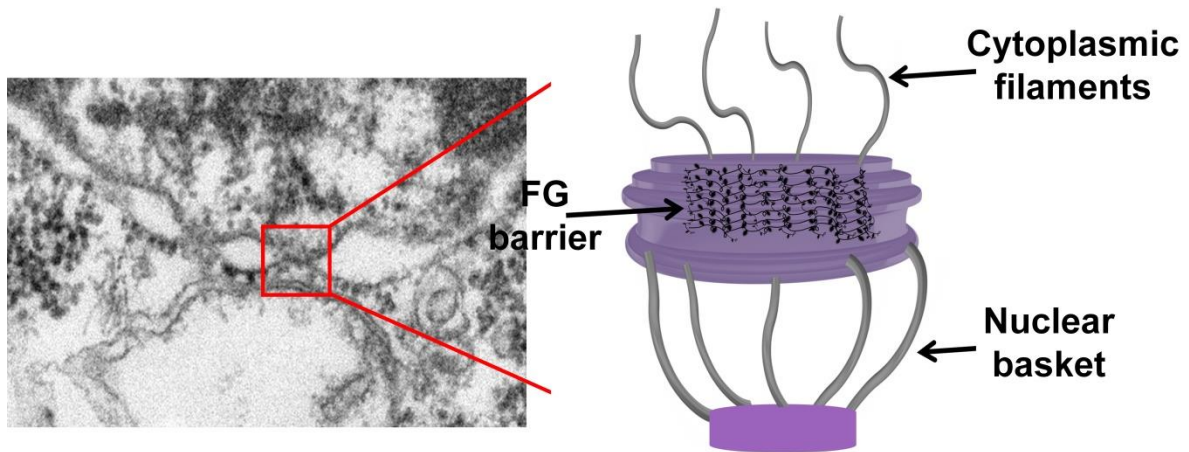


Figure 1. Nuclear pore complex structure. (a) Schematic of the nuclear pore complex basic structure.

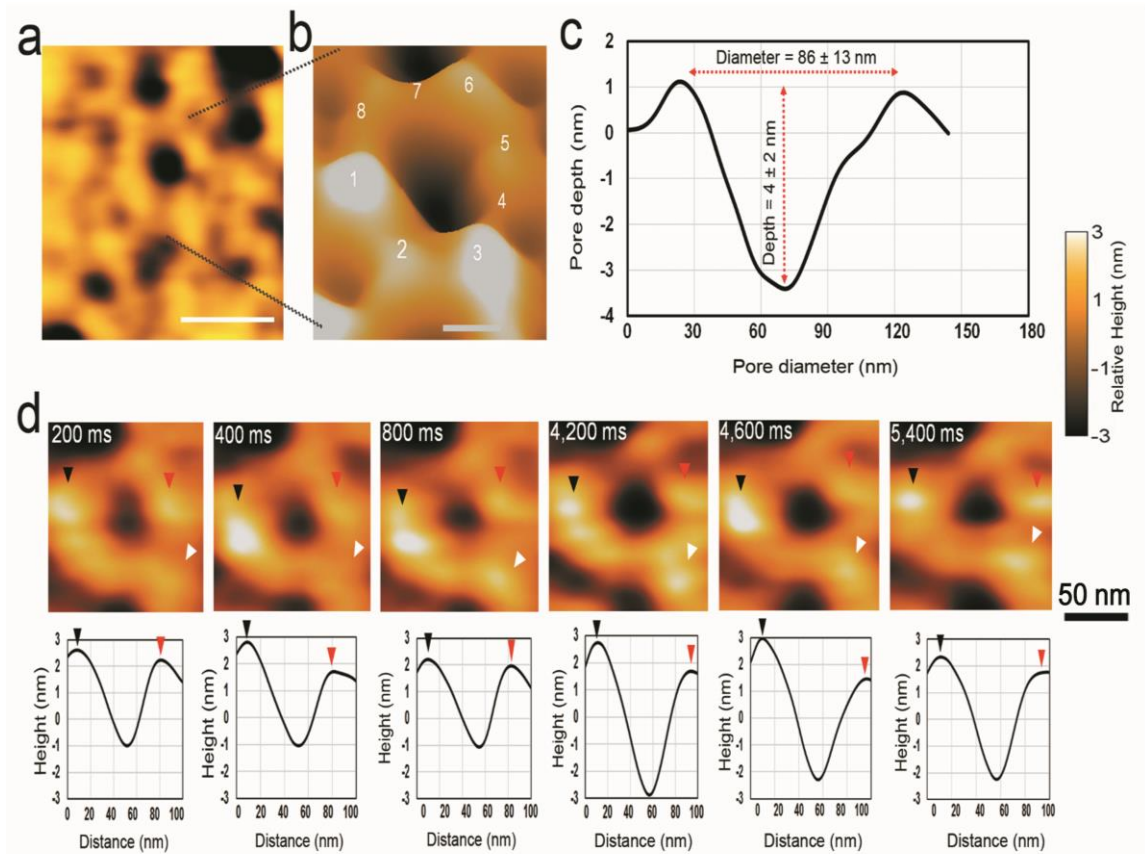


Figure 2. HS-AFM observation of native human NPCs. This is HS-AFM images recorded from the native samples to show the NPC intact structure and live dynamics of the cytoplasmic face.

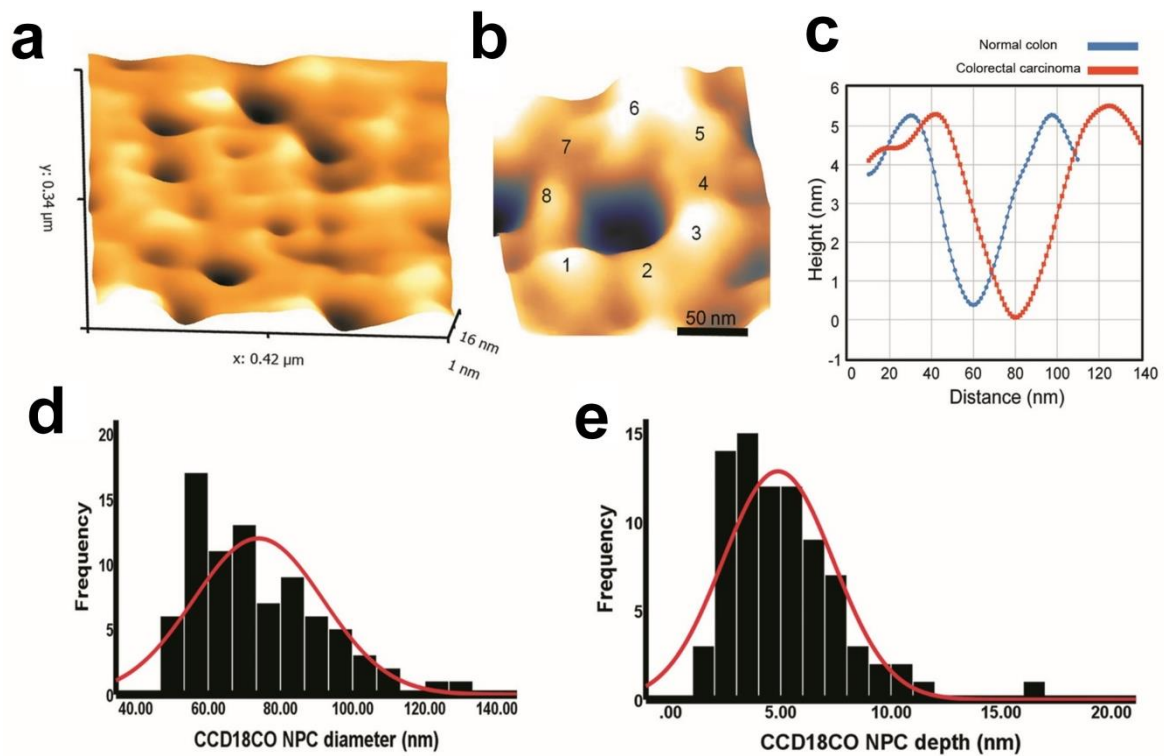


Figure 3. HS-AFM observation of native NPCs of normal colon cells. (a) HS-AFM image showing of the cytoplasmic face of the native nuclear envelope of CCD18CO cells. Z-range = 16 nm, scanning speed is 2 frame per second. (b) HS-AFM image rendered to 3D format showing average structure native NPCs appeared in **a**. (c) Plot showing the average diameter and depth of NPC as 74 ± 18 nm and 5 ± 2.5 nm respectively (N=81). The average diameter is a little smaller than colorectal cancer NPCs. (d) Normal distribution curve of NPC diameter. (e) Normal distribution curve of NPC depth

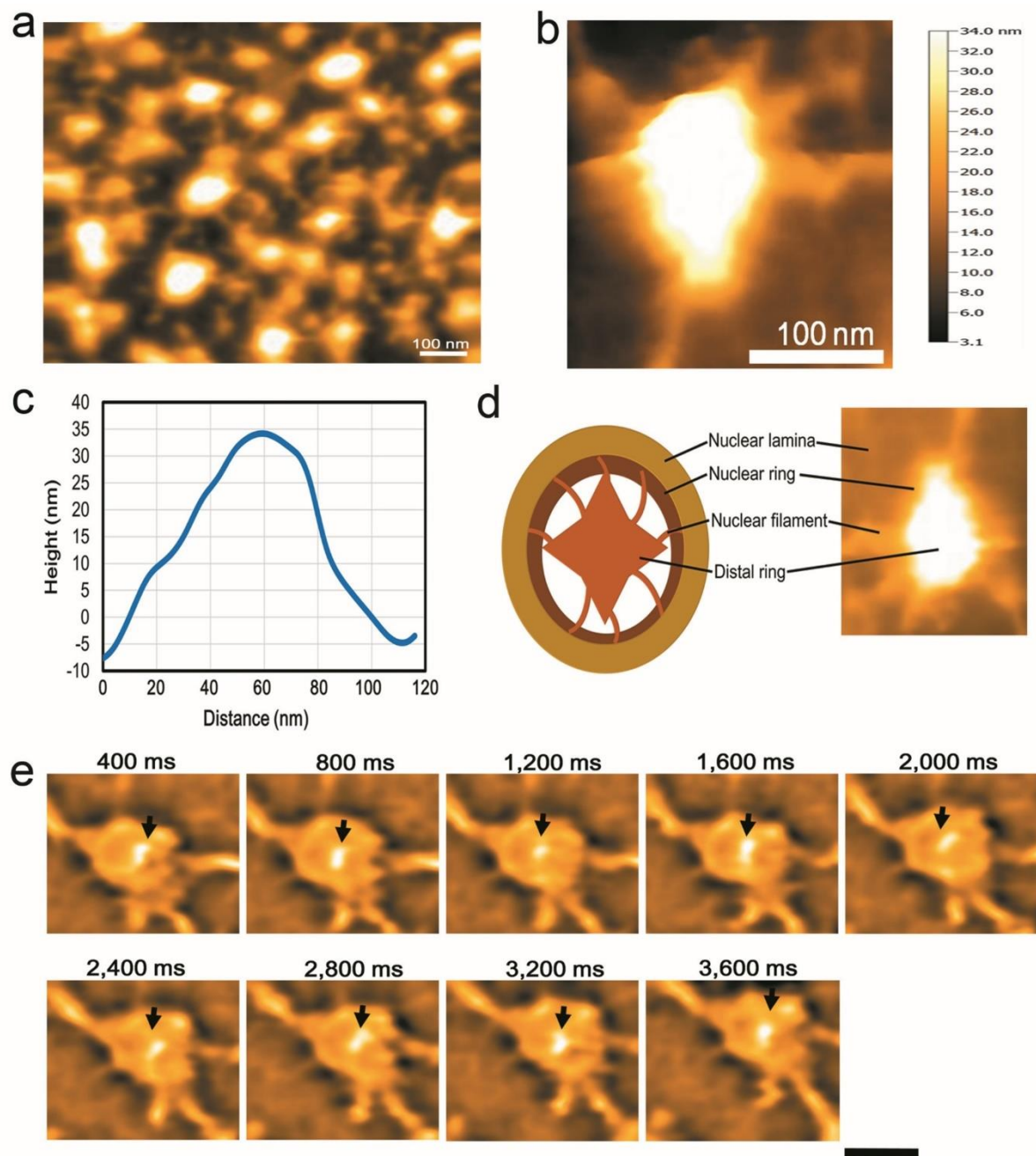


Figure 4. HS-AFM observation of native nuclear basket dynamics in HCT116 cells.

(a) HS-AFM image of 600×600 nm scan area showing the native nuclear baskets of colorectal cancer cells. Z-range = 34 nm, scanning speed is 2.5 frame per second. (b) HS-AFM image rendered in 3D format showing a single native native nuclear basket with stretched nuclear filaments surrounding the distal ring. Z-range = 34 nm, scanning speed is 2.5 frame per second. (c) Average diameter of native nuclear basket $\sim 102 \pm 23$ nm and the average height $\sim 34 \pm 6$, (N=27). (d) Illustration showing the structure of the nuclear basket protruding from the nuclear lamina. The HS-AFM observations showed the average thickness of the native nuclear ring $\sim 12 \pm 2.8$, (N=20). (e) HS-AFM images showing the rapid changes of the distal ring (black arrow) together with the nuclear filaments of a native nuclear basket. Z-range = 34 nm, scanning speed is 2.5 frame per second.

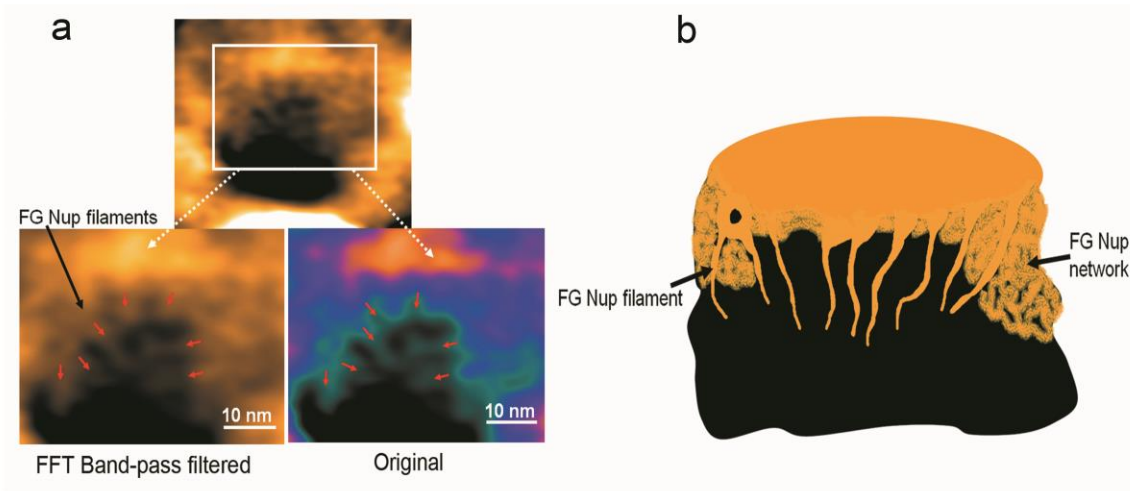


Figure 5. Live tracking of FG-Nups inside the inner channel. (a) HS-AFM frame magnified to show extended FG-Nup threads tethered from the NPC inner ring. (b) Diagram illustrating the FG-Nup threads in (b) showing their extension inside the central channel.

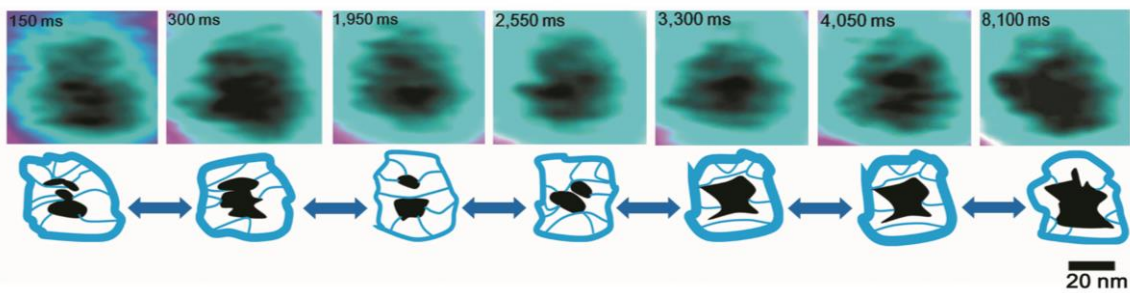


Figure 6. FG Nup-Cobweb conformational sequential conformations. HS-AFM images showing an extension of the FG-Nups analysis in (Figure 23). A $40 \times 40 \text{ nm}^2$ area (Z-scale = 19 nm) of the central channel was imaged using the higher speed of 6.7 frames/s to show the behavior of the FG-Nups network. Different frames show conformational changes of FG threads retracting and diffusing and sometimes forming a network that looks like a cobweb.

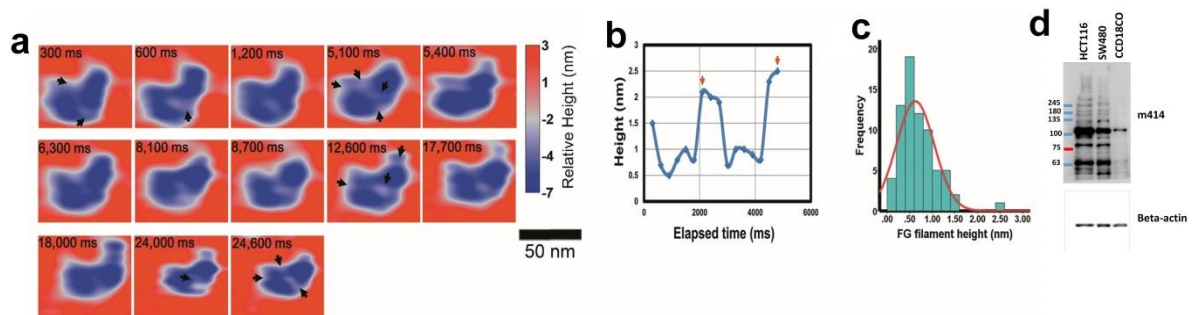


Figure 7. FG-IDP single filament-tracking in normal colon native NPCs. (a) This HS-AFM recorded images showing a low density of FG Nup filaments inside the central channel. (b) Cross-sections showing the heights of single FG filaments over the elapsed time. (c) Normal distribution curve showing the mean value of FG Nup height. (d) Western blot analysis showing the protein levels of some FG Nups (m414) in both cancer and normal colon cells.

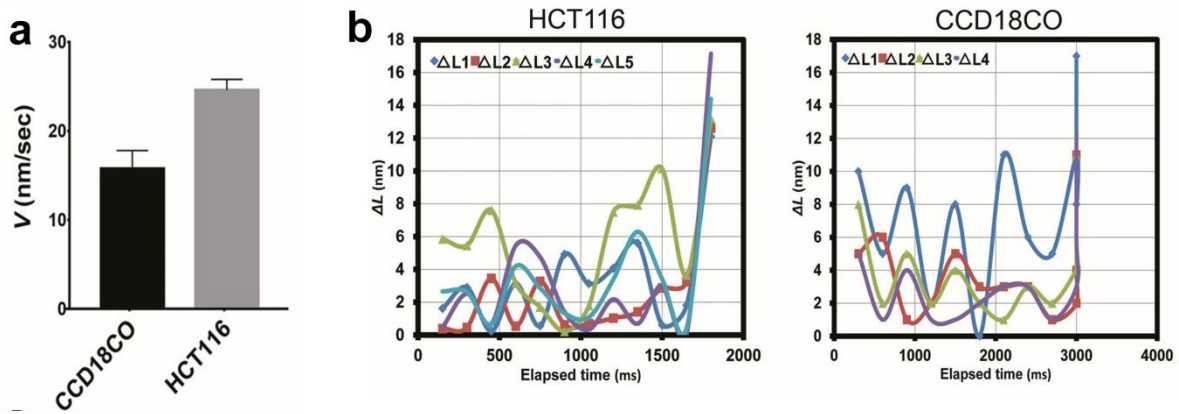


Figure 8. Single FG filament extension velocity. (a) Individual FG filament length-change velocity measured by calculating the length-change over different time points. (b) Graphs showing FG filament length-change over elapsed time in both cancer and normal cells.

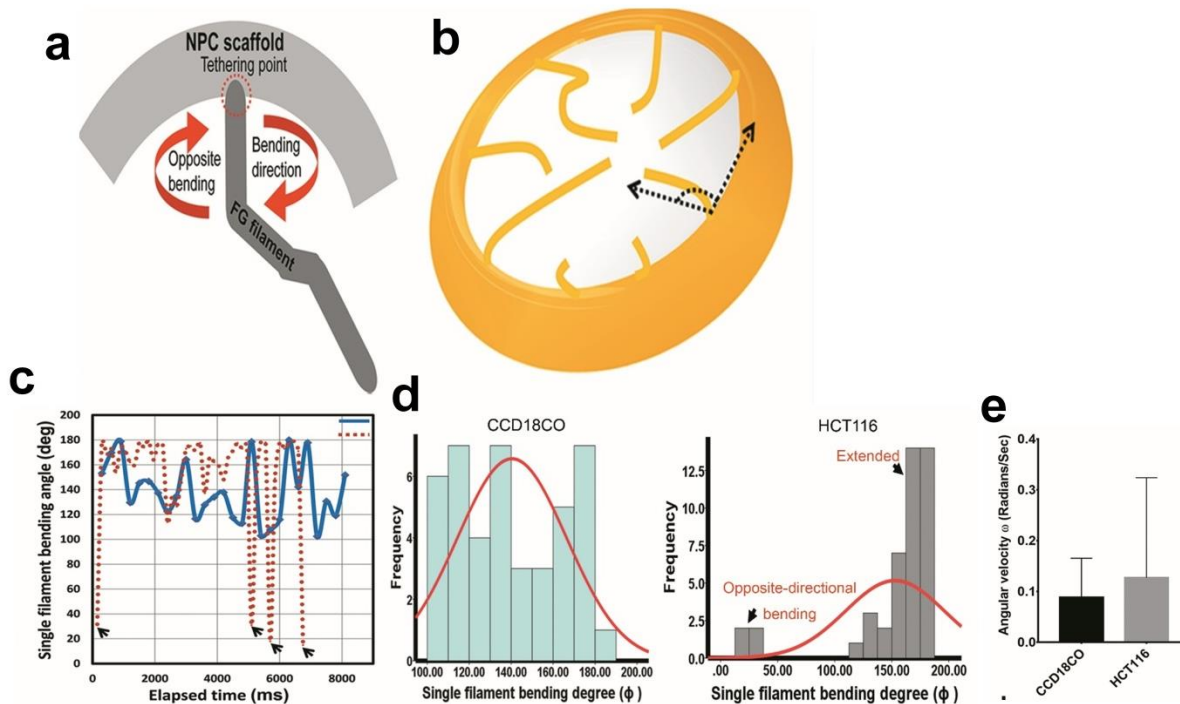


Figure 9. Bending abilities of single FG filaments measured in normal and cancer. (a) Diagram showing the bending possibilities of FG Nup filaments in two different directions away from their tethering points. (b) The angle measurements shown in the diagram on the right; shows the extending and retracting FG filaments inside the central channel of NPC. (c) FG Nup filament bending angle plotted against the elapsed time to track the bending of single filaments away from the scaffold NPC. Black arrows indicate some points the bending happened at the opposite direction of all other bending points. (d) Shows the normal distribution curve of FG Nup filament bending angle in CCD18CO and HCT116. (e) A plot showing the angular velocity of individual FG filaments in both CCD18CO and HCT116 as calculated from the same filaments shown in c.

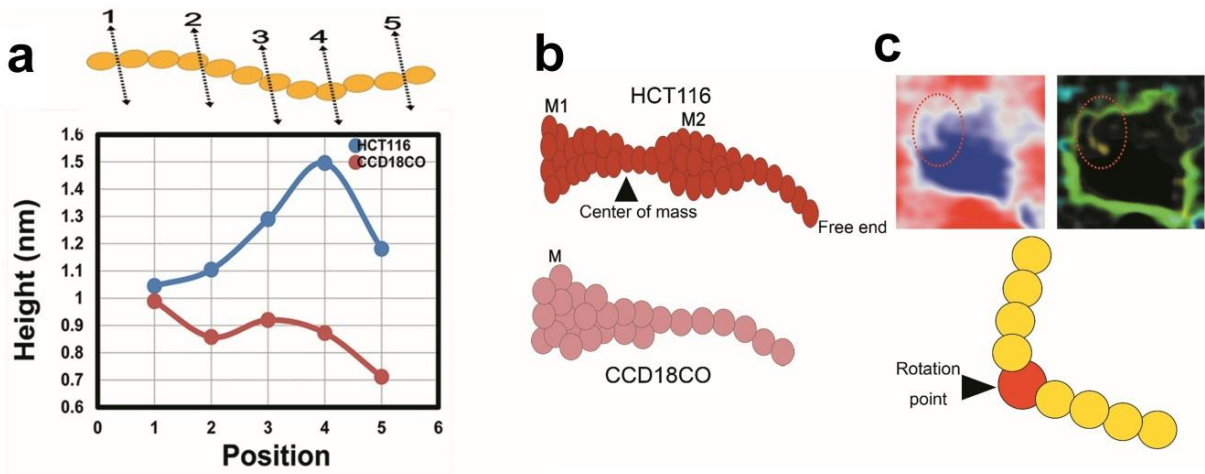


Figure 10. Single FG filament bending model. (a) FG filaments entire length dissection. (b) FG filament dissection result schematic showing thick points working as a rotation points. (c) HS-AFM representative image of single FG filaments captured in HCT116 NPCs.

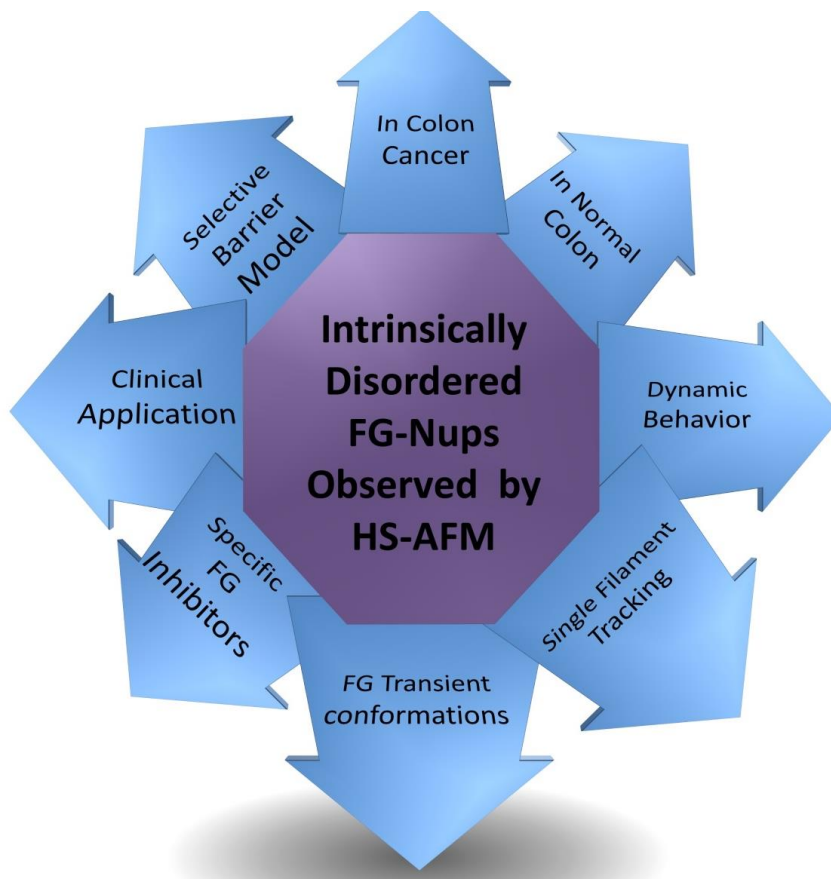


Figure 11. HS-AFM resolved FG Nups behaviour. Diagram showing different IDP-FG Nup unknown characteristics that could be partially resolved by HS-AFM in the current study.

Discussion and Conclusions

HS-AFM has been developed and used for the visualization of biomolecules in dynamic action at a high spatiotemporal resolution without disturbing their normal function; however, the observation of live dynamics of intracellular organelles, such as the nucleus or mitochondria, is still very challenging due to cantilever tip sizes and morphologies, intact sample buffering and immobilization techniques, measurement conditions, and other nano-mechanical parameters. Here, unlike with other conventional snapshots or static measurements of “averaging-out” imaging techniques, we directly visualized intact cytoplasmic faces of NPCs in normal and cancer colon cells (Figure 1-3) and nuclear baskets by HS-AFM in their native environments (Figure 4). Our HS-AFM observations showed that FG-Nups have a wriggle brush-like shape, and we further speculated a “spiders/spidermen working inside the entangled cobweb” model for the process of central channel transport or gene gating by the nuclear pore complex. FG Nups native dynamics in colorectal cancer cells resolved as shown in Figure 5, 6. The density and distribution of FG Nups in normal colon cells appeared to be lower than cancer cells in terms of FG Nup filaments number and protein levels as shown in Figure 7.

The NPC selective barrier is believed to be an integral overall meshwork, and chasing NPCs in their native working environment should give a better understanding of FG-Nup behaviour and of how they compose the flexible selective barrier. Here, we propose an alternative cobweb-like model (Figure 6) which dealing with some of the neglected factors by other previous models, and our study differs from previous studies in several points. First, we resolved the behaviour of native NPCs from human colon cancer cells, which have a selective central barrier. Second, we considered that the flexible motions of FG-Nup filaments inside the NPC channel are likely to be strongly affected by their tethering

origins and interactions with the other scaffolding Nups located at the NPC rim. Third, our data determine that the FG-Nup filaments can change their thickness over time, which suggests a different mechanism from those proposed in the previous studies. Fourth, our HS-AFM live recordings showed the contributions by the behaviour of FG-Nup filaments within an existing central granule, for which most biophysical and dynamic deep details have yet to be investigated.

There are growing evidences that a wide range of cellular activities highly connected to tumorigenesis are dependent on the organization of the NE and NPC. Therefore, how the morphology of NE/NPCs change in normal/healthy cells when they become tumour cells may directly contribute to tumorigenesis understanding. My current study of FG Nup patterns and dynamic behaviour in normal and cancer cells contribute not only to understanding their principal biomedical characteristics but also to developing promising diagnostic and therapeutic tools for colorectal cancer ([Figure 8-10](#)). Furthermore, Due to the technical limits, IDP-FG single filament motions and dynamics still explained by the term of random motion or Brownian motion, because these single nano-filaments are highly dynamic, disordered and invisible in vitro. Thus, my current model is the a typical tentative biophysical model explaining the bending, extension and dynamic behaviour of single IDP-FG filaments in healthy and cancer cells based on typical experimental approaches. Therefore, my current model might open the door for many future advanced approaches to track the IDP-FG complexes in different species ([Figure 11](#)).

学位論文審査報告書（甲）

1. 学位論文題目（外国語の場合は和訳を付けること。）

Probing the Spatial-temporal Properties of the Nuclear Pore Complex（核膜孔複合体の時空間特徴の解明）

2. 論文提出者 (1) 所 属 自然システム学 専攻

(2) 氏 名 MAHMOUD SHAABAN MOHAMED ABDELRASOUL

3. 審査結果の要旨（600～650 字）

核膜孔複合体 (NPC) は核膜に存在する核内外の物質輸送を担う唯一のゲートであり、ナノマシンとして機能している。NPC はヌクレオポリン(Nups)と呼ばれる約 30 種類のたんぱく質で構成され、その約 30%はネイティブで二次構造を取りにくいフェニルアラニン・グリシンリピートヌクレオポリン (FG-Nups) であり、輸送選択性に関与している。これまでに様々な方法で NPC 構造が可視化されてきたが、全て静的なスナップショットであり、NPC 構造のダイナミクスについて言及したものはなかった。本学位論文は、高速原子間力顕微鏡 (HS-AFM) を用いて、大腸がん細胞の FG-Nups 及び核膜孔の中心プラグ構造のダイナミクスを直接的に可視化、解析したものである。申請者は再発がん臨床試験で使用されているアポトーシス及びオートファジー誘導物質である MLN8237/alisertib で大腸がん細胞を処理し核膜孔を観察した所、Nups の機能低下、特に FG-Nups の選択的バリアの変形と喪失を見出し、これががん細胞が死に至るコードの一つであると結論付けた。さらに申請者は HS-AFM で二次構造を取りにくい (IDP)・FG フィラメントを正常細胞とがん細胞において観察・解析し、がん細胞特異的に高い弾性曲げ運動が見られることを明らかにした。さらに、特定の条件下で核膜孔の中心プラグ構造となり得る、IDP-FG フィラメントが徐々に凝集体を形成する様子の撮影に成功した。これらネイティブ状態における NPC と FG Nups のリアルタイムダイナミクスを明らかにした成果があることから、本研究が博士（理学）に値するものと評価した。

4. 審査結果 (1) 判 定 (いずれかに○印) 合格 ・ 不合格

(2) 授与学位 博士（理学）